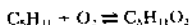


## DIRECT MEASUREMENTS OF THE NEOPENTYL PEROXY-HYDROPEROXY RADICAL ISOMERISATION OVER THE TEMPERATURE RANGE 660-750 K

KEVIN J. HUGHES, PETER A. HALFORD-MAW, PHILLIP D. LIGHTFOOT,  
TAMÁS TURÁNYI AND MICHAEL J. PILLING  
*School of Chemistry, University of Leeds, Leeds LS2 9JT, U.K.*

The rate constant for the isomerisation reaction  $\text{neo-C}_5\text{H}_{11}\text{O}_2 \rightarrow \text{C}_5\text{H}_{10}\text{OOH}$  ( $k_3$ ) has been determined directly over the temperature range 660-750 K.  $\text{neo-C}_5\text{H}_{11}\text{I}$  was photolysed at 248 nm using a KrF laser in the presence of  $\text{O}_2$  and He. The alkyl radical generated in the photolysis reacts with  $\text{O}_2$  to form the peroxy radical which then isomerises to the hydroperoxy radical. Subsequent rapid reactions lead to the generation of OH, which was detected by laser induced fluorescence as a function of time. At high  $[\text{O}_2]$  the time constant,  $\lambda$ , for the build up of OH tends to  $-k_1$ . As  $[\text{O}_2]$  decreases, earlier reactions in the peroxy radical chain become important and analysis of the  $[\text{O}_2]$  dependence of  $\lambda$ , allows both  $k_1$  and  $k_2$ , the rate constant for the peroxy radical decomposition, to be determined. Data analysis shows that the results are fully compatible with the steady-state measurements of Baldwin *et al* except that values for  $k_1$  a factor of over ten lower than their values are obtained. The discrepancy is shown to be due to errors in the equilibrium constant,  $K_2$ , they used for the (R2) reaction.



An Arrhenius analysis gives

$$(k_1/s^{-1}) = 10^{12.2-0.077} \exp\{-(1.48 \pm 0.12) \times 10^4 \text{K}/T\}$$

The measurements of  $k_2$  were combined with literature data for  $k_3$  and calculated values of  $\Delta S_2^\ddagger$  to give  $\Delta H_2^\ddagger(298) = 142 \pm 6 \text{ kJ mol}^{-1}$  for the  $\text{neo-C}_5\text{H}_{11} + \text{O}_2 \rightleftharpoons \text{C}_5\text{H}_{11}\text{O}_2$  equilibrium, in satisfactory agreement with group additivity values.

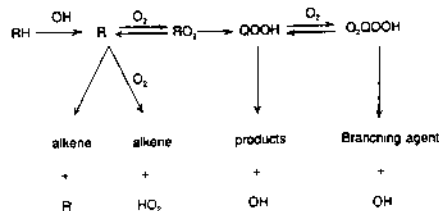
### Introduction

The elucidation of the mechanism of knock in a gasoline engine and the provision of a quantitative assessment of the propensity of a fuel to knock remain important goals in combustion chemistry. Although autoignition occurs at high temperatures (>900 K), there is strong evidence that lower temperature chemistry is significant through the generation of heat and reactive species.<sup>1</sup> This lower temperature mechanism involves peroxy radicals and the dependence of the kinetics on the structure of the precursor alkyl radicals has been the subject of much discussion. Morley, in particular, has demonstrated good correlation between Blending Research Octane Number (BON) and the kinetics of the production of the branching agent in the peroxy radical chain.<sup>2</sup>

The overall mechanism for the low temperature oxidation of hydrocarbons is summarised in Scheme I. Morley argued that any analysis of autoignition propensity should examine those features of the combustion mechanism that affect the numbers of radical centres i.e. initiation, termination and the

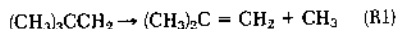
generation of the branching agent. Initiation is generally accepted as of minor mechanistic consequence and termination is little affected by alkane structure. The key characteristic of a fuel which provides a link between molecular structure and knock propensity is the peroxy radical chain outlined in Scheme I. Within this scheme, the isomerisation reaction,  $\text{RO}_2 \rightarrow \text{QOOH}$ , which involves intramolecular hydrogen atom transfer, was identified by Morley as the primary, structure-re-

SCHEME I Outline mechanism for low temperature hydrocarbon combustion

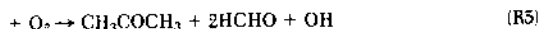
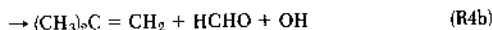
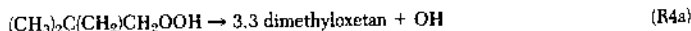
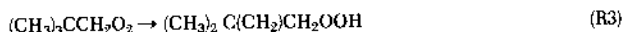
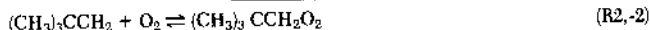


lated step in his correlation with BON. Keck has also discussed the relationship between fuel sensitivity to knock and peroxy radical isomerisation.<sup>3,4</sup>

The available rate data on peroxy radical isomerisation were determined by Baldwin, Walker and coworkers using steady-state techniques with end product analysis.<sup>5</sup> Their seminal work may be summarised by referring to neo-pentane as fuel, which has the twin advantages that all H atoms are equivalent and that it cannot react with O<sub>2</sub> to generate an alkene (Scheme I). Baldwin *et al.*<sup>5</sup> generated the neo-pentyl radical by adding small amounts of neo-pentane to a slowly reacting H<sub>2</sub> + O<sub>2</sub> system. Decomposition of the radical generates isobutene:



while the formation of the peroxy radical generates 3,3-dimethyloxetan (DMO) isobutene and acetone via the sequence:



A steady-state analysis was used to show that, after correction for isobutene formation in (R4b), the relative product yields are given by:-

$$\frac{[\text{Acetone}] + [\text{DMO}]}{[\text{i-butene}]} = \frac{K_2 k_3 [\text{O}_2]}{k_1} \\ = R[\text{O}_2].$$

They combined their end product analysis studies with Arrhenius parameters for  $k_1$ <sup>5,6</sup> and bond additivity estimates of  $K_2$ <sup>7</sup> to determine  $k_3$  for a wide range of alkanes and hence to formulate general rules for calculating rate constants for internal H atom transfer in RO<sub>2</sub> radicals from the alkyl radical structure. It was these rules that Morley used in his BON correlations.<sup>2</sup>

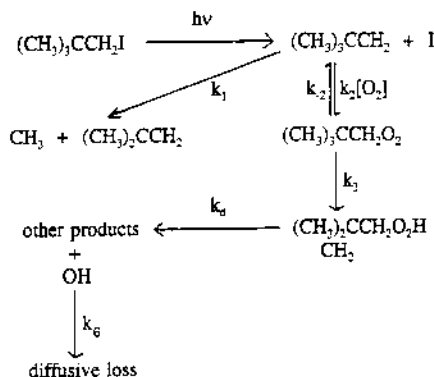
More recently, Gutman and coworkers have measured the peroxy radical equilibrium constants,  $K_2$ , directly for several alkyl radicals.<sup>8</sup> Their experiments resulted in substantial revisions of the group additivity values with  $K_2$  increasing, in some cases, by more than a factor of 10. These increases, in turn, require a decrease in the estimates of  $k_3$ , although no such general revision has been performed. Clearly direct measurements of  $k_3$  are needed, which do not rely on other parameters. The

aim of the present paper is to report such measurements for the neo-pentyl radical.

The basis of the technique is shown in Scheme II; it is a time-resolved equivalent of the classic Baldwin-Walker mechanism. The radical is generated by flash photolysis of neo-pentyl iodide and reacts via a mechanism involving (R1), (R2,-2) and (R3). The reactions of the hydroperoxy radical ((R4) and (R5) in the scheme of Baldwin *et al.*) are fast and non-rate-determining and lead to the generation of OH, which can be sensitively detected by laser induced fluorescence (LIF). Provided (R3) is the rate-determining step in this sequence, its rate constant can then be related to the rising portion of the OH LIF signal, the decay being determined by the slow diffusive loss of OH from the monitoring zone and reaction with C<sub>5</sub>H<sub>11</sub>I ( $k_6$ ). A key to the success of the technique is the use of low precursor and radical concentrations, so that both radical-radical and radical-molecule reactions, other than those

contained within Scheme II, are minimised. At the temperatures studied ( $T \approx 750$  K), the methyl radicals generated in reaction (R1) react with O<sub>2</sub> to produce CH<sub>3</sub>O<sub>2</sub> and less than 1% form HCHO + OH.<sup>9</sup>

### Scheme II



### Experimental

The reaction vessel was a heated stainless steel cell, based on a design described in detail elsewhere.<sup>10</sup> The cell has three optical axes, mutually at right angles, fitted with a total of 5 spectrosl windows sealed with water-cooled 'O' rings. Two of the axes were used for the photolysis and probe laser beams, whilst the fluorescence was detected in the third, vertical axis by a photomultiplier (EMI 9813QKB) which faced the pumping port. Light access to the photomultiplier was via a focussing lens, slit and interference filter centred on 308 nm. The reaction vessel was heated by four 400 W high density cartridge heaters (Watlow Firerod) embedded in the cell walls. The temperature was monitored and controlled by two chromel-alumel type K thermocouples (Thermocoax) inserted inside the reaction vessel above and below the observation region. The flow of gases through the cell was controlled by three calibrated mass flow controllers (Tylan FC-280) through which helium, oxygen and a C<sub>5</sub>H<sub>11</sub>I/He mixture were flowed. The overall flow rate was controlled by an exit needle valve and the pressure inside the reaction vessel was monitored by capacitance manometers (MKS Baratron, 0–10<sup>5</sup> and 0–10<sup>4</sup> Torr). The oxygen pressure was varied between 2 and 250 Torr and the helium diluent pressure between 400 and 1500 Torr.

A Lambda Physik LPX 105i excimer laser, operating at 248 nm on KrF, was employed as the photolysis source and a Nd:YAG pumped frequency doubled dye laser (Spectron Laser Systems SL800) was used as the probe laser. Typical excimer pulse energies were 50–200 mJ, with a shot to shot variation of <5%. The Nd:YAG laser was operated at 282.323 nm on the Q<sub>1</sub>(3) line of the A<sup>2</sup>Σ<sup>+</sup>(v = 1) – X<sup>2</sup>Π(v = 0) transition. Typical concentrations were [C<sub>5</sub>H<sub>11</sub>I] = 7 × 10<sup>12</sup> cm<sup>-3</sup> and [OH]<sub>max</sub> = (1–5) × 10<sup>11</sup> cm<sup>-3</sup>. The intensity of each laser shot was monitored directly for each laser beam by directing them, after leaving the reaction vessel, on to cuvettes filled with dye solution: the intensities of the resulting fluorescence signals were measured using photodiodes. The signals from the photodiodes and the photomultiplier were captured by a three channel, gated sample and hold system and stored, via an analogue to digital converter, on a microcomputer which also controlled the timing sequences of the lasers and the sample and hold system. Data collection and processing consisted of defining a total number of time points, at predefined delays relative to the photolysis laser, with a given number of samples at each time point. Typically 100 time points were employed with 10–500 μs interpoint times and 30–50 samples at each time point. The firing of the lasers was then controlled so as to access these samples randomly. When data collection

was completed, each fluorescence signal was normalised to the excimer laser and doubled dye laser signals and an average taken of the samples at each time point. The temporal profile was analysed by non-linear least squares fitting (see below).

### Results

A typical fluorescence temporal profile is shown in Fig. 1. The decay corresponds to diffusive loss of OH and reaction with C<sub>5</sub>H<sub>11</sub>I, as confirmed both from its temperature and pressure dependences and from independent experiments in which OH was generated at 193 nm from N<sub>2</sub>O/H<sub>2</sub>O/He mixtures. Analysis of the profile confirms a biexponential form:

$$[\text{OH}]_t = A \exp(\lambda_+ t) + B \exp(-k_6 t)$$

If reaction (R3) is the rate determining step in the sequence generating OH, then  $-\lambda_+ = k_3$  and  $\lambda_-$  should be independent of [O<sub>2</sub>] and of total pressure. Figure 2 demonstrates that  $\lambda_-$  depends sensitively on [O<sub>2</sub>] showing that this presumption is incorrect. At low [O<sub>2</sub>],  $k_2[\text{O}_2]$  and  $k_3$  become comparable and (R1-3) must be recognised within the reaction scheme. Under these conditions, the time-dependence of OH is given by:

$$[\text{OH}]_t = \alpha \{ -(\lambda_+ + k_6) \exp(\lambda_+ t) + (\lambda_- + k_6) \exp(\lambda_- t) + (\lambda_- - \lambda_+) \exp(-k_6 t) \}$$

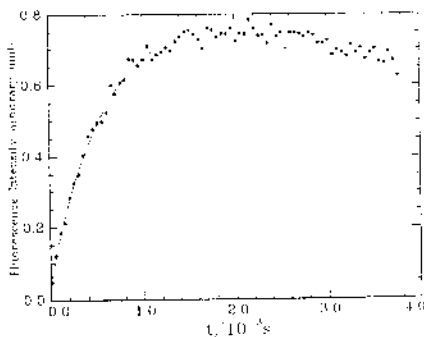


FIG. 1. Time dependence of the OH LIF signal following photolysis of neo-pentyl iodide at 248 nm. ●, experimental results (average of 50 shots); — non-linear least squares fit to a biexponential time dependence. [C<sub>5</sub>H<sub>11</sub>I] = 7 × 10<sup>12</sup> cm<sup>-3</sup>, [C<sub>5</sub>H<sub>11</sub>I]<sub>0</sub> = 3 × 10<sup>11</sup> cm<sup>-3</sup>, T = 700 K, helium pressure = 550 Torr, oxygen pressure = 63.3 Torr,  $-\lambda_+ = (156 \pm 80 \text{ s}^{-1})/\alpha$ ,  $k_6 = (88 \pm 10 \text{ s}^{-1})/\alpha$ .

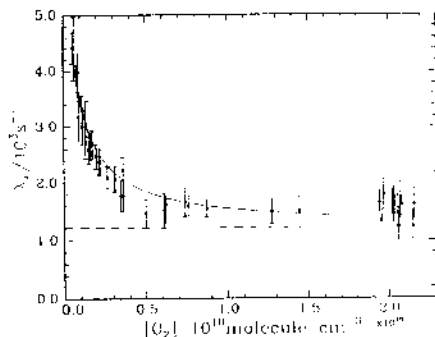


FIG. 2. Plot of  $\lambda$ , obtained from biexponential fits to the OH profiles versus  $[O_2]$ ,  $T = 700$  K, helium pressure = 550 Torr. ●, experimental results with 95% confidence limits; —, non-linear least squares fit using eqn (2) with  $k_{-2}$  and  $k_3$  as variable parameters. ----, limit as  $[O_2] \rightarrow \infty$ , where  $\lambda \rightarrow -k_3$ .

where

$$\alpha = \frac{k_2 k_3 [C_5H_{11}][O_2]}{(\lambda_+ - \lambda_-)(\lambda_+ + k_6)} \quad (1)$$

and

$$\lambda_- = \frac{-\beta \pm (\beta^2 - 4\gamma)^{1/2}}{2} \quad (2)$$

where

$$\beta = k_1 + k_2[O_2] + k_{-2} + k_3$$

and

$$\gamma = k_1 k_{-2} + k_1 k_3 + k_2 [O_2] k_3$$

$\lambda_+$  and  $\lambda_-$  are both negative.

Under the experimental conditions employed  $|\lambda_-| \gg |\lambda_+|$ ,  $k_6$  so that the term in  $\exp(\lambda_- t)$  is negligible and eqn (1) reduces to a biexponential with the exponential term in  $\lambda_+ t$  describing the build up of OH and that in  $k_6 t$  describing the decay.  $\lambda_+$  varies with  $[O_2]$  tending to  $-k_3$  at high  $[O_2]$  and to  $-(k_{-2} + k_3)$  as  $[O_2]$  tends to zero. The full kinetic system (R1–R6) was examined using numerical integration. Good agreement was found with the simple biexponential function.

Figure 2 demonstrates that  $|\lambda_+|$  shows the required dependence on  $[O_2]$ , decreasing as the oxygen pressure is increased and tending to a high oxygen limit. There is insufficient information contained in the  $[O_2]$  dependence of  $\lambda_+$  to determine all four rate parameters,  $k_1$ – $k_3$ , from a fit to this dependence. However,  $k_1$  has recently been measured directly by Slagle *et al.*<sup>11</sup> over the temperature range 560–650 K; they reported Arrhenius parameters for the high pressure limiting rate constant and a means of describing the pressure dependence. Similarly Xi *et al.*<sup>12</sup> have measured  $k_2$  between 266 and 374 K, giving  $k_2 = 2.1 \times 10^{-12} (T/300 \text{ K})^{-2.1} \text{ cm}^3 \text{ molecule}^{-1} \text{ s}^{-1}$ . These data were used to provide estimates of  $k_1$  and  $k_2$  under the present experimental conditions and Fig. 2 shows a fit to the data using equation (2) with  $k_{-2}$  and  $k_3$  as variable parameters. Table I lists the resulting rate parameters. It was not possible to determine  $k_{-2}$  at low temperatures because (R3) remains the rate-determining step even at the lowest  $[O_2]$  employed and the high oxygen concentration asymptote applies throughout. It also proved difficult to obtain reliable data at low  $[O_2]$  at 750 K because

TABLE I  
Experimental values for  $k_{-2}$  and  $k_3$

$T/K$	$k_{-2}/s^{-1}$	$k_3/s^{-1}$	$k_3/s^{-1}$ (Baldwin <i>et al.</i> ) <sup>11</sup>
660	—	$(2.96 \pm 0.33)^b \times 10^2$	$3.82 \times 10^2$
670	—	$(3.33 \pm 0.38) \times 10^2$	$5.29 \times 10^2$
690	$(7.14 \pm 1.35)^b \times 10^3$	$(8.49 \pm 1.67) \times 10^2$	$9.87 \times 10^2$
700	$(7.59 \pm 0.54) \times 10^3$	$(1.23 \pm 0.09) \times 10^3$	$1.33 \times 10^3$
715	$(1.11 \pm 0.11) \times 10^4$	$(1.64 \pm 0.25) \times 10^3$	$2.05 \times 10^3$
730	$(1.90 \pm 0.35) \times 10^4$	$(2.05 \pm 0.33) \times 10^3$	$3.11 \times 10^3$
750	—	$(4.12 \pm 0.81) \times 10^3$	$5.26 \times 10^3$

<sup>a</sup>From the Arrhenius expression  $k_3 = 1.2 \times 10^{13} \exp(-120 \text{ kJ mol}^{-1}/RT) \text{ s}^{-1}$ .

<sup>b</sup>The quoted errors are the 95% confidence limits determined directly from the data analysis. See text for a further discussion.

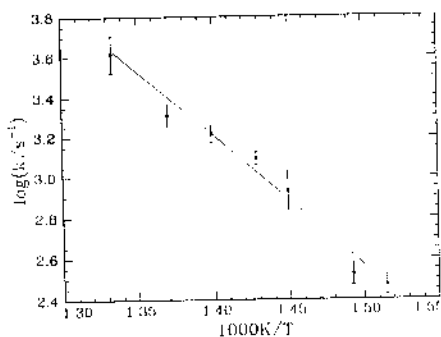


FIG. 3. Arrhenius plot for  $k_3$ . The error bars represent 95% confidence limits.

of limitations in the time resolution of the detection system, so no value of  $k_{-2}$  is reported at this temperature either.  $k_3$  was primarily determined from the approach to the high  $[O_2]$  asymptote.  $k_{-2}$ , by contrast, depends on the increase in  $[A_1]$  at low  $[O_2]$  and is more sensitive to the input parameters, the more inaccurate of which is  $k_2$ , because of the need to extrapolate the expression of Xi *et al*<sup>12</sup> to higher temperatures. The uncertainty in  $k_{-2}$  could be as large as a factor of 2.

Figure 3 shows an Arrhenius plot for  $k_3$  and gives

$$k_3/s^{-1} = 10^{12.2 \pm 0.77} \exp\{-1.48 \pm 0.12\} \times 10^4 K/T\}$$

where the errors are the  $1\sigma$  values. The A factor is in good agreement with Benson's estimate.<sup>13</sup> The activation energy,  $(123 \pm 10) \text{ kJ mol}^{-1}$ , is the sum of the activation energy for H abstraction by a peroxy radical and the strain energy for the ring. Taking the data of Walker *et al*<sup>14</sup> for  $HO_2 + C_2H_5$  ( $E_a = 85.6 \text{ kJ mol}^{-1}$ ) as a model requires a strain energy of  $(37 \pm 10 \text{ kJ mol}^{-1})$  which is surprisingly high for a six membered ring.

## Discussion

The directly measured values of  $k_3$  are compared in Table I with the values calculated from the Arrhenius expression recommended by Baldwin *et al*.<sup>5</sup> The two sets of rate constants differ by more than a factor of 10. The dependence of  $\lambda_1$  on  $[O_2]$  allows us to probe further into the origin of his discrepancy. The directly measured quantity in the experiments of Baldwin *et al* was the ratio  $R = K_2 k_3/k_1$ . Table II shows the values of R calculated from the values of  $k_3$  and  $k_{-2}$  determined in the present experiments, together with the literature values of  $k_1$  and  $k_2$ . R was determined in two ways, from the experimental values themselves and from the best fit Arrhenius expression for  $k_3$ . Given the uncertainties in  $k_{-2}$  and  $k_3$  and in the literature values of  $k_1$  and  $k_2$ , the agreement is excellent: the experimental results reported by Baldwin *et al*<sup>5</sup> are in full agreement with those reported here. The discrepancies arise from the values of  $k_1$  and  $k_2$  employed by Baldwin *et al* to calculate  $k_3$  from their experimental measurements of R and, primarily,

TABLE II

A comparison of the experimental values of  $R = K_2 k_3/k_1$  and of the parameters  $K_2$  and  $k_1$  from the present work and from that of Baldwin *et al*<sup>5</sup>

T/K		$R/10^{-13} \text{ cm}^3 \text{ molecule}^{-1} \text{ s}^{-1}$ (c)		$K_2/10^{-17} \text{ cm}^{-3}$ (e)	$k_1/10^4 \text{ s}^{-1}$ (f)
690	(a)	4.02		5.11	1.08
	(b)		4.29	0.407	1.01
700	(a)	3.85		4.66	1.49
	(b)		3.23	0.313	1.39
715	(a)	2.11		3.05	2.37
	(b)		2.15	0.215	2.20
730	(a)	0.95		1.71	3.69
	(b)		1.46	0.149	3.41

a: This work

b: Baldwin *et al*

c: From the data reported in Table I (for (a) data set)

d: From the  $k_{-2}$  values reported in Table I and the Arrhenius expression for  $k_1$  (for (a) data set)

e:  $K_2 = k_2/k_{-2}$  with  $k_2$  taken from Xi *et al*<sup>12</sup> (for (a) data set)

f:  $k_1$  calculated from the Arrhenius expression for the high pressure limit of Slagle *et al* (for (a) data set)

from  $K_2$ . Table II presents a comparison. The values of  $k_1$  are in generally very good agreement while those of  $K_2$  differ by more than an order of magnitude, fully accounting for the difference in the final estimates of  $k_3$ . The assumption has been made in the analysis that reaction (R3) is irreversible under the experimental conditions. The relative thermodynamic stability of  $RO_2$  and  $QOOH$  requires that  $k_{-3} > k_3$ , so that irreversibility is only guaranteed if  $k_{eff} = k_4 + k_5[O_2]\delta \gg k_{-3}$ . (The factor of  $\delta$  allows for reversibility in reaction (R5)). The evidence for the latter inequality derives from the work of Baldwin *et al.*<sup>5</sup> Further work is in progress to test the validity of this inequality using the present system.

It is pertinent to compare the present results, with the equilibrium constants,  $K_2$ , of Slagle *et al.*<sup>5</sup> They did not study the neopentyl radical, but, within the limits of group additivity, our results may be compared with their data for  $C_2H_5$  (the three methyl H atoms in  $C_2H_5$  are replaced by  $CH_3$  groups on both reactant and product sides of the  $R + O_2 \rightleftharpoons RO_2$  equilibrium). The most appropriate comparison is to calculate  $\Delta H_2^\circ(298)$ , the enthalpy change of reaction (R2), which can be effected, following Slagle *et al.*,<sup>8</sup> through a Third Law calculation:

$$RT \ln K_p(T) + X = - \frac{\Delta H_2^\circ(298)}{RT} + \frac{\Delta S_2^\circ(298)}{R}$$

where  $X$  represents the temperature dependences of  $\Delta H^\circ$  and  $\Delta S^\circ$  and depends on  $\Delta C_p$ .  $\Delta S_2^\circ(298)$  was equated to the value used by Slagle *et al.*<sup>6</sup> for the  $C_2H_5$  equilibrium  $-150.2 \text{ J mol}^{-1} \text{ K}^{-1}$  and the small correction factor,  $X$ , was also taken from their paper. These values are derived from estimates made by Wagner and Melius<sup>15</sup> of the structures and internal motions of  $C_2H_5$  and  $C_2H_5O_2$ , which were based on experimental studies, *ab initio* calculations and analogies with stable compounds. Table III shows the values for  $\Delta H_2^\circ(298)$  at the four experimental temperatures. The mean value of  $-142 \pm 6 \text{ kJ mol}^{-1}$  agrees well with the measurement of Slagle *et al.*<sup>6</sup> of  $-147 \pm 6 \text{ kJ mol}^{-1}$ , based on direct observation of the approach to equilibrium in the  $C_2H_5 + O_2 \rightleftharpoons C_2H_5O_2$  system and the same value for  $\Delta S_2^\circ(298)$ . As pointed out by Slagle *et al.*, group additivity estimates give  $\Delta H^\circ(298) = -136 \text{ kJ mol}^{-1}$  for the  $C_2H_5$  reaction, provided the currently accepted 'higher' value for  $\Delta H_f^\circ(C_2H_5)$  is employed. They argued that their results require a reduction of  $8 \text{ kJ mol}^{-1}$  for the O-C(O) group heat of formation, although such a change would lead to a disparity in the comparison of experimental and group bond enthalpies for  $C_3H_5O_2$  where previously good agreement has been found.<sup>14</sup> The present results, on the other hand, show reasonable agreement with the group additivity values and

TABLE III

Enthalpies of reaction for  $C_5H_{11} + O_2 \rightleftharpoons C_5H_{11}O_2$ , calculated from the experimental values of  $K_2$  using a Third Law method.

T/K	$-\Delta H_2^\circ(298)/\text{kJ mol}^{-1}$	
	a	b
690	140.6	132.2
700	142.3	133.5
715	142.7	133.9
730	141.8	133.0

a: Calculated from  $K_p$  using  $\Delta S_2^\circ(298)$  derived from the estimates of Wagner and Melius for  $C_2H_5$ .

b: Calculated from  $K_p$  using group additivity estimates of  $\Delta S_2^\circ(298)$ .

suggest that such a revision is unnecessary. This agreement is further improved if  $\Delta S_2^\circ(298)$  is calculated using group additivity (Table III) which gives a mean value for  $\Delta H_2^\circ(298)$  of  $133 \pm 6 \text{ kJ mol}^{-1}$ . However, the indirect nature of the present determination of  $k_{-2}$ , and the consequent  $\pm 6 \text{ kJ mol}^{-1}$  uncertainty in  $\Delta H_2^\circ(298)$ , require that any conclusions regarding the group heat of formation are treated with caution. We are attempting to determine  $\lambda_{-2}$  at lower  $[O_2]$ , where  $k_{-2}$  is better defined.

### Conclusions

1. The rate constant,  $k_3$ , for the isomerisation reaction  $C_5H_{11}O_2 \rightleftharpoons C_5H_{11}OOH$  has been determined over the temperature range 660–750 K, giving  $\log(k_3/s^{-1}) = (12.2 \pm 0.77) - (122.7 \pm 10.3) \text{ kJ mol}^{-1}/2.303 RT$ .
2. The oxygen dependence of the rate of OH production has allowed the determination of  $k_{-2}$ , the rate constant for decomposition of  $C_5H_{11}O_2$ , to be determined over the temperature range 690–730 K.
3. Combining  $k_{-2}$  with the data of Xi *et al.*<sup>9</sup> for the forward reaction,  $k_2$ , allows  $\Delta H_2^\circ(298)$  to be calculated from the equilibrium constant  $K_2$  using a Third Law method. A value of  $142 \pm 6 \text{ kJ mol}^{-1}$  is obtained, in reasonable agreement with both the results of Slagle *et al.*<sup>6</sup> and with group additivity calculations.<sup>5,6</sup>
4. The results of the time dependent studies of OH production are in excellent agreement with the experimental results of Baldwin *et al.* obtained using steady-state techniques. The values obtained for  $k_3$  are, however, over a factor of ten lower than their values. This difference can be ascribed entirely to their use of an inaccurate value for the equilibrium

constant,  $K_2$ , in calculating  $k_3$  from their experimental results.

#### Acknowledgements

This work was performed as part of the EC JOULE CHEMCOM program. We thank the Royal Society and the Hungarian Academy of Science for a Visiting Fellowship for TT.

#### REFERENCES

- WESTBROOK, C. K. AND PTZ, W. J.: SAE872107.
- MORLEY, C.: *Combust. Sci. Tech.*, 55, 115 (1987).
- KECK, J.: SAE 872110
- KECK, J.: Twenty-Third International on Symposium Combustion, p. 455 The Combustion Institute, 1988.
- BALDWIN, R. R., HISHAM, M. W. M. AND WALKER, R. W.: *J. Chem. Soc. Faraday Trans. 1*, 78, 1615 (1982).
- BALDWIN, R. R., WALKER, R. W. AND WALKER, ROBERT W.: *J. Chem. Soc. Faraday Trans. 1*, 76, 825 (1980).
- BENSON, S. W. AND SHAW, R.: *Organic Peroxides*, (D. Swern, Ed.) Vol. 1, p 105, Wiley (New York) 1970.
- SLACLE, I. R., RATAJCZAK, E. AND GUTMAN, D.: *J. Phys. Chem.*, 90, 402 (1986).
- BAULCH, D. L., COBOS, C. J., COX, R. A., FRANK, P., JUST, TH., KERR, J. A., PILLING, M. J., TROE, J., WALKER, R. W. AND WERNATZ, J.: *J. Phys. Chem. Ref. Data* (in press).
- BROCARD, M., MACPHERSON, M. T. AND PILLING, M. J.: *J. Phys. Chem.*, 93, 4043 (1989).
- SLACLE, I. R., BATT, L., GMURCZYK, G. W., GUTMAN, D. AND TSANG, W.: *J. Phys. Chem.*, 95, 7732 (1991).
- XI, Z., HAN, W. J. AND BAYES, K. D.: *J. Phys. Chem.*, 92, 3450 (1988).
- BENSON, S. W.: The mechanism of pyrolysis, oxidation and burning of organic compounds, NBS Special Publication, 357, US Dept Commerce, Washington DC, 121 (1972).
- WALKER, R. W., HONEYMAN, M. R., DEAN, C. E. AND BALDWIN, R. R.: *J. Chem. Soc. Faraday Trans., 2*, 82, 89 (1986).
- WAGNER, A. F. AND MELIUS, C. F.: cited in reference 6.
- MORGAN, C. A., PILLING, M. J., TULLOCH, J. M., RUIZ, R. P. AND BAYES, K. D.: *J. Chem. Soc. Faraday Trans. 2*, 78, 1323 (1982).

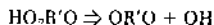
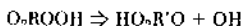
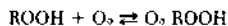
#### COMMENTS

Joseph W. Bozzelli, *New Jersey Institute of Technology, USA*. The apparent ring strain of 37 KJ/mole for isomerization ( $R_1$ ) of the neopentyl-peroxy radical to the hydroperoxy seems quite high for a 6 member ring. Is there a possibility that the rate constant you are measuring is actually a combination of the two steps in the reaction sequence, i.e. isomerization and then reaction to products forming the OH radical you are monitoring. If this is the case you may also need to include R-3 or the equilibrium constant,  $K_1$ , in your kinetic analysis. The endothermicity of (R3) reduces the  $E_a$  of (R-3) by ca. 52 KJ/mole corresponding to the difference in the primary C-H bond cleaved and a hydroperoxy ROO-H bond formed. This combined with an  $A_{-3}$  of only  $10^{10}$ /sec (100 times lower than forward isomerization  $A$  factor), leads to a reverse rate some 40 times faster than the forward at 700 K.

*Author's Reply*. We agree that  $k_{-1} \gg k_1$ . However, Baldwin et al. (Reference 5) used their product spectrum to estimate  $k_{-1}$ ,  $k_{10}$  and  $k_5$ . Their analysis shows that  $(k_{-1} + k_{10} + k_5 [O_2]) \gg k_{-1}$  at all oxygen concentrations studied here. Thus  $C_5H_{10}OOH$ , once generated, reacts rapidly and reverse isomerisation is unimportant. It should be recalled that our experimental results are fully compatible with those of Baldwin et al. and the

difference in our conclusions can be traced to the value of  $K_2$  employed. There is, therefore, no inconsistency in the use of their results to establish the above inequality, which does not depend on  $K_2$ .

William J. Pittz, *Lawrence Livermore National Laboratory, USA*. The "dihydroperoxide" path proposed by Benson:



where  $R = C_5H_{10}$  and  $R' = C_5H_9$ .

If this "dihydroperoxide" path is fast, two OH radicals will result for each neopentyl radical consumed.

*Author's Reply*. Our technique is independent of the stoichiometry  $C_5H_{10}OOH \rightarrow fOH$ , provided  $f$  is unchanged over the experimental OH profile. The low radical concentration ensures that first-order reactions dominate, and any contributions from radical-radical reactions, which could affect the pro-

file if branching occurred, are negligible. Thus, if there are reactions in the mechanism subsequent to the isomerisation that lead to the generation of more or less than one OH per  $C_7H_{16}OOH$  radical, the analysis is unaffected.

•

*J. F. Griffiths, University of Leeds, U.K.* Did you have particular reasons for studying the neopentyl peroxy radical? Are there prospects (or specific plans) to extend the study of this important class of reactions to species involving the longer chain alkyl radical moieties?

*Author's Reply.* The neopentyl radical was the subject of an earlier extensive study by Baldwin et

al. (Reference 5 in the text). There are two additional advantages. Firstly the hydrogen atoms available for internal abstraction are all equivalent, so that only one type of peroxy-hydroperoxy radical isomerisation is feasible. Secondly, there are no  $\beta$ -C-H bonds which simplifies the reaction mechanism. In particular, the reaction of the radical with  $O_2$  cannot generate the alkene +  $HO_2$ . We are currently extending this study to the ethyl radical, although ethene +  $HO_2$  presents some problems. We also plan to study n-propyl, using D-substitution to identify the atom abstracted. Extension to larger alkanes may prove too complex, but our aim is to investigate the validity of the experimental results of Baldwin et al. and then recall their values, if appropriate. Such a procedure should enable us to provide estimates for larger radicals.